



Universiteit
Leiden
The Netherlands

Vulvar squamous cell carcinoma : genetics, morphology and clinical behaviour

Trietsch, M.D.

Citation

Trietsch, M. D. (2017, November 9). *Vulvar squamous cell carcinoma : genetics, morphology and clinical behaviour*. Retrieved from <https://hdl.handle.net/1887/54945>

Version: Not Applicable (or Unknown)

License: [Licence agreement concerning inclusion of doctoral thesis in the Institutional Repository of the University of Leiden](#)

Downloaded from: <https://hdl.handle.net/1887/54945>

Note: To cite this publication please use the final published version (if applicable).

Cover Page



Universiteit Leiden

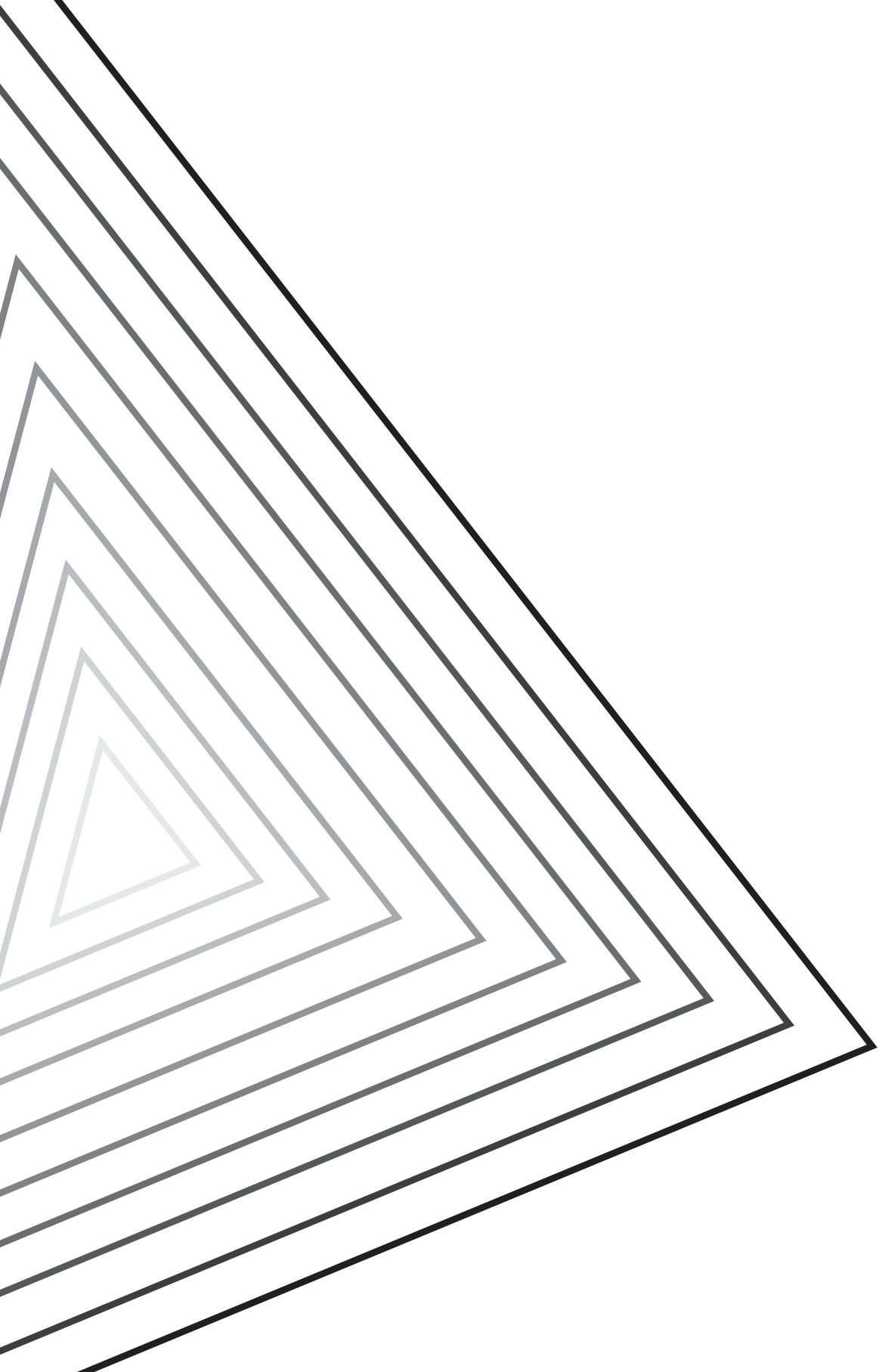


The handle <http://hdl.handle.net/1887/54945> holds various files of this Leiden University dissertation.

Author: Trietsch, M.D.

Title: Vulvar squamous cell carcinoma : genetics, morphology and clinical behaviour

Issue Date: 2017-11-09



Chapter 7

Targeted sequencing of primary, metastatic and recurrent spindle cell variant vulvar cancer reveals a highly heterogeneous genetic disease

Marjolijn D Trietsch, Nalini Siewnath, Natalja T ter Haar, Willem E Corver, Gert Jan Fleuren

Abstract

Vulvar squamous cell carcinoma (VSCC) patients can suffer from rapid progression and recurrence. A higher risk of lymph node metastases and worse survival has been attributed to VSCCs with spindle cell morphology. To determine whether the spindle cell component is the origin of metastasis, we analyzed the mutational status of 66 primary VSCCs and their spindle cell components, lymph node metastases, and recurrences.

Mass spectrometry screening was performed for 13 relevant genes (*BRAF*, *CDKN2A*(p16), *CTNNB1*, *FBXW7*, *FGFR2*, *FGFR3*, *FOXL2*, *HRAS*, *KRAS*, *NRAS*, *PIK3CA*, *PPP2R1A* and *PTEN*). Solid components of VSCCs with and without spindle cell morphology were also screened for mutations in *TP53*.

TP53, *CDKN2A* and *HRAS* were most frequently mutated. Mutational profiles differed from the primary tumor in 64% of lymph node metastases and 81% of recurrences. There was no difference in mutation frequency between VSCCs with and without spindle cell morphology (77 vs 58%, NS). Spindle cell components were more likely to have the same profile as adjacent solid components (86% of cases).

Our study reveals that VSCCs likely consist of multiple, genetically different, clones. There is no proof of a selective role for somatic mutation(s) in the onset of spindle cell morphology. VSCCs with spindle cell morphology have a higher risk of lymph node metastasis and a worse 5-year survival. However, based on the mutational spectra, we have not been able to identify spindle cell components as the origin of metastasis or recurrence. Our findings could be of importance when developing targeted therapy.



Introduction

Vulvar cancer is a relatively rare gynecological malignancy, with approximately 2 new cases per 100,000 women each year (9;15;18;22). It is mostly seen in post-menopausal women, with an average age at diagnosis of 70 years. The most prevalent subtype of vulvar cancer is squamous cell carcinoma (VSCC), but other types such as basal cell carcinoma and melanoma also occur. VSCC is known to develop through two different etiologic pathways (8;34). The first pathway is clearly associated with infection by oncogenic high risk human papilloma viruses (HPV) and is mainly seen in younger patients. HPV produces proteins E6 and E7 that interact with the tumor suppressor proteins p53 and pRB (37), resulting in loss of wild-type function. The second pathway, which usually affects older patients, develops independent from HPV infection, and is associated with the chronic skin condition lichen sclerosus (3;33;34). HPV-negative VSCCs often carry somatic mutations in, amongst others, the *TP53* gene (30). The HPV dependent and the HPV independent pathway differ greatly in onset, but they do share a key role of p53.

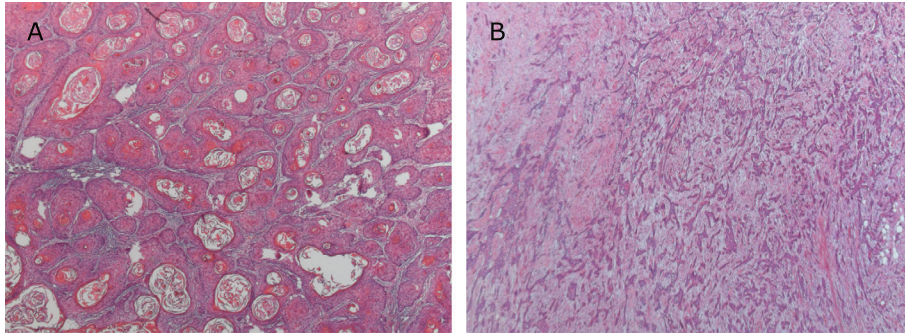
Although surgical treatment is curative in most early stage cases, some patients suffer from rapid progression and recurrence (2;6;11) due to yet unknown reasons. In higher staged VSCC, radiotherapy and chemotherapy can be applied, but these treatment modalities have high morbidity rates (11). It is important to find risk factors that can help clinicians to identify those patients that are most at risk of progressive or recurrent disease, but to date the presence of lymph node metastases is the only accurate prognostic factor for survival and recurrence (12;20).

Approximately 20% of VSCCs have a subpopulation of cells with a distinct type of morphology called 'spindle cell morphology'. This subgroup of, almost exclusively HPV negative, VSCCs has a tumor component with loose, elongated tumor cells budding from the invasive front of the tumor. VSCCs with spindle cell morphology (VSCC-S) have a higher risk of lymph node metastasis and a worse 5-year survival when compared to VSCC that consist of a 'solid' component alone (31). (Figure 1)

The etiology of vulvar spindle cell morphology is not yet fully understood. Spindle shaped epithelial tumor cells seem to have lost part of their epithelial characteristics, and gain mesenchymal traits and metastatic capacities, known as epithelial-to-mesenchymal transition (EMT) (1;16). These metastatic capacities are reflected by the fact that VSCC-S have a higher risk of lymph node metastases (31). It is thought that changes in the TGF β pathway might play a role in the onset of EMT and spindle cell morphology (26), but other molecular or genetic processes such as somatic mutations may also be of importance. Although it is a plausible hypothesis, it has not been proven that the spindle shaped cells are the origin of metastasis and recurrences, or that the tumor as a whole has gained aggressive traits.



Figure 1 Vulvar squamous cell carcinoma with spindle cell morphology



Representative images of vulvar squamous cell carcinoma (A) and vulvar squamous cell carcinoma with spindle cell morphology (20x magnification) (B).

In this study, we have compared the mutational profile of VSCCs with and without spindle cell morphology to gain insight in the recurrence and metastatic process of VSCC-S. We used the genetic alterations as identifiers to recognize a progressive pathway from solid primary tumor to spindle cells, which in term might be the origin of lymph node metastases and recurrences.

Methods

Patients

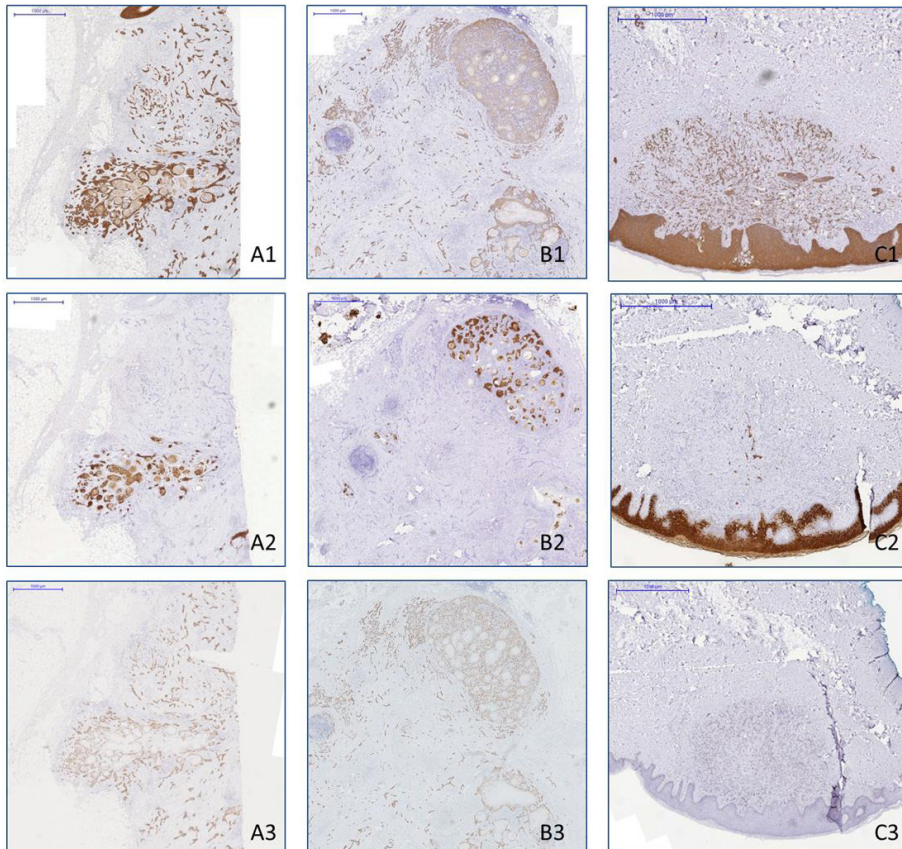
All patients that were surgically treated for primary VSCC in the Leiden University Medical Center between 2000 and 2010 were selected. All tissue samples were screened for mutations and spindle cell morphology before (31;32). Clinical follow up data were examined up to December 2012. Patients who were surgically treated for recurrence or lymph node metastasis within this follow up period were included in this study. Patient samples were handled according to the Code of Conduct for Proper Secondary Use of Human Tissue of the Dutch Federation of Biomedical Scientific Societies.

Identification of spindle cell morphology

All surgically removed recurrences and lymph nodes from the patients that were selected as described above, were screened for spindle cell morphology on all available tissue blocks. In short, 4 μ m sections were cut from paraffin embedded, formalin fixed tumor tissue blocks, and stained for pankeratin, keratin 10 and keratin 14, respectively (27) clones AE1/AE3, MAB3412, 1:2000, Millipore, Billerica, Massa-



Figure 2 Figure showing immunohistochemical staining of primary, lymph node and recurrence with spindle cell morphology



Tissue taken from the primary tumor (A), the lymph node metastasis (B) and the recurrence (C) of the same vulvar squamous cell carcinoma patient, stained for pancytokeratin (1), cytokeratin 10 (2) and p53 (3). Note the presence of both spindle cell morphology and solid tumor in the lymph node metastasis. Spindle cells can be distinguished from 'normal' VSCC cells by the presence of pancytokeratin staining (1), and the absence of cytokeratin 10 staining (2). Slides 3 are stained for p53 and show a mutational staining pattern in all three tissue specimens.



achusetts, USA; DE-K10, 1:50, DAKO Glostrup, Denmark; and LL002, 1:2000, Abcam, Cambridge, UK). Spindle cell morphology was determined as described before (31). In short: loose, elongated cells with a minimum distance of 0.5 mm to the solid component of the tumor and with a positive staining for pankeratin and keratin 14, but negative for keratin 10 were marked as spindle cells. Figure 2 shows an example of the expression of these proteins in a VSCC with spindle cell morphology.

DNA Isolation and FACS

The stained tissue slides were used to select and mark solid and spindle cell regions. The marked areas were transferred to the corresponding FFPE tissue blocks. Next, 4 - 5 0.6 mm diameter tissue cores were taken from the selected areas and transferred into a micro vessel.

DNA from solid tumor component tissue cores was isolated using a Tissue Preparation System (Siemens Healthcare Diagnostics, Malvern, Pennsylvania, USA) as described previously (14). The tissue cores were carefully punched from solid tumor tissue to prevent high amount of 'contamination' with stromal tissue.

Spindle cell morphology has a diffuse growth pattern in which spindle shaped cells are frequently intermingled with other types of tumor and normal infiltrating cells. This has consequences for further downstream genetic analysis using total DNA extracts. To circumvent this problem we used multiparameter fluorescence-activated cell sorting (FACS) to obtain pure tumor subpopulations using a dissociation protocol (4) with modifications that allowed the simultaneous analysis of pan-keratin, keratin 10, keratin 14, vimentin and DNA content.

Tissue cores from spindle cell morphology areas were cut into small pieces and were dewaxed using xylene, and were rehydrated. Next, tissues were subjected to heat-induced, antigen retrieval (HIAR) by heating the samples to 80°C in 10 mM sodium citrate buffer for 60 minutes. Samples were digested for 60-90 minutes at 37°C in a 0.1% mixture of collagenase and dispase in Rosswell Park Memorial medium (RPMI), with intermitted grinding at 15 minute intervals using the GentleMACS tissue grinder (protocol spleen 03_02) (Miltenyi Biotec, Bergisch Gladbach, Germany). When samples were sufficiently digested and the solution gained a cloudy appearance, samples were washed in PBA-Tween and filtered through an 80 µm mesh filter. Cell concentration was determined using the Muse Cell Analyzer (Merck Millipore, Darmstadt, Germany). 10^6 cells were incubated overnight at 4°C with 50 µL of primary antibody. Next day, samples were washed in PBA-Tween and incubated with a mixture of secondary goat anti-mouse subclass specific fluorescently labelled antibodies on ice for 60 minutes. Labelling concentrations and manufacturers are stated in Table 1. Cells were washed with NST buffer. (146 mM NaCl, 10 mM Tris-HCl, pH 7.5, 1 mM CaCl₂, 0.5 mM MgSO₄, 21 mM MgCl₂, 0.05% bovine serum albumin, 0.2% Nonidet P40 (Sigma)) with 4,6-diamidino-2-phenylindole (DAPI; 10 µM (Sigma)) For every 10^6 cells, 0.5mL (10 µM) of DAPI in NST buffer was incubated in the dark at 4°C for at least 2 hours.

Flow cytometric analysis was performed using an LSRII flow cytometer (BD Biosciences, San Jose, CA). A UV 355 nm, blue 488 nm and the red 635 nm laser were used for excitation. DAPI, FITC, R-PE, APC and APC-Cy7 fluorescence were collected using the following band pass filters, respectively: 450/50 nm, 530/30 nm, 572/25 nm, 670/14 nm and 780/60 nm. Diva 6.3.1 software was used for acquisition. Data files containing information from at least 50,000 single cell events were analyzed using ModFit 4.0, remotely linked to WinList 8.0 (Verity software House, Topsham, ME).



Table 1 Antibody concentrations

primary antibody	clone	isotype	concentration	company	secondary antibody	concentration	company
pankeratin	Ks pan 1-8	IgG2A	1:5	Acris Antibodies, Herford, Germany	APC	1:200	SBA, Birmingham, AL, USA
keratin 10	DE-K10	IgG1	1:5	DAKO, Glostrup, Denmark	FITC	1:100	SBA, Birmingham, AL, USA
keratin 14	LL002	IgG3	1:100	Abcam, Cambridge, UK	APC-Cy7	1:100	SBA, Birmingham, AL, USA
vimentin	V92b	IgG2B	1:50	ARA, Alphen a/d Rijn, the Netherlands	RPE	1:200	SBA, Birmingham, AL, USA
DNA					DAPI		

APC allophycocyanin
 FITC fluorescein isothiocyanate
 RPE R-phycoerythrin
 DAPI 4',6-diamidino-2-fenylindool

Table 2 Staining patterns

	solid	spindle cells	stromal tissue
pankeratin	+	+	-
keratin10	+	-	-
keratin14	+	+	-
vimentin	-	+/-	+
DNA	+	+	+

For sorting, a FACSaria III was used equipped with a 50 mW 407 nm violet laser, a 20mW 488nm blue laser, a 50 mW 561 green laser and an 18 mW 635 red laser. For fluorescence collection the same filter settings were used as in the LSRII. Tumor cells were sorted using a 100 µm nozzle at 20 psi and a drop frequency of 31.2 kHz and a purity precision sorting mode (purity mask: 16, yield mask: 16). Three types of tumor subpopulations were isolated: spindle cells, tumor cells from the solid component and stromal cells, each having their own characteristic staining pattern (table 2). DNA isolation of the sorted cells was performed as described before (7) followed by DNA purification (NucleoSpin Tissue kit, Machery-Nagel, Germany).



Mutation analysis

MALDI-TOF

All samples were screened for hotspot mutations using the GynCarta 2.0 MALDI-TOF Mass Spectrometry panel (28). This panel contains the most relevant loci for gynecological malignancies on 13 different genes (*BRAF*, *CDKN2A*(p16), *CTNNB1*, *FBXW7*, *FGFR2*, *FGFR3*, *FOXL2*, *HRAS*, *KRAS*, *NRAS*, *PIK3CA*, *PPP2R1A* and *PTEN*, see Supplemental table 3 for specific mutations). Data was analyzed by two investigators separately with MassARRAY Typer Analyser software (TYPER 4.0.22, Sequenom, Hamburg,

Table 3 Somatic mutations in solid components of VSCC

Patient	primary	lymph node	recurrence
1	TP53 + CDKN2A + PTEN	TP53 + CDKN2A	TP53 + CDKN2A
2	CDKN2A	WT	<i>na</i>
3	TP53 + KRAS	<i>na</i>	WT
4	TP53	<i>na</i>	TP53
5	TP53	<i>na</i>	TP53
6	TP53	WT	<i>na</i>
7	HRAS	<i>na</i>	CDKN2A
8	TP53	<i>na</i>	<i>na</i>
9	WT	TP53	<i>na</i>
10	WT	WT	WT
11	TP53 + PIK3CA + HRAS	HRAS	<i>na</i>
12	TP53° + CDKN2A	TP53° + CDKN2A	<i>na</i>
13	TP53	<i>na</i>	<i>na</i>
14	WT	<i>na</i>	TP53
15	WT	<i>na</i>	WT
16	WT	<i>na</i>	WT
17	TP53	<i>na</i>	WT
18	TP53 + HRAS	WT	<i>na</i>
19	WT	WT *	TP53 + CDKN2A
20	WT	TP53	<i>na</i>
21	CDKN2A + HRAS	<i>na</i>	<i>na</i>
22	TP53	WT	<i>na</i>
23	TP53 + CDKN2A	<i>na</i>	<i>na</i>
24	TP53	<i>na</i>	<i>na</i>
25	TP53	TP53	<i>na</i>
26	WT	<i>na</i>	<i>na</i>
27	CDKN2A	WT	WT
28	TP53	<i>na</i>	failed*
29	WT	<i>na</i>	failed*
30	TP53 + PIK3CA + HRAS	WT *	<i>na</i>
31	TP53	<i>na</i>	WT
32	TP53	WT	<i>na</i>
33	PIK3CA + PPP2R1A	<i>na</i>	PIK3CA
34	TP53 + HRAS	TP53 + HRAS	<i>na</i>
35	TP53°	<i>na</i>	TP53°
36	WT	WT	<i>na</i>
37	TP53	<i>na</i>	WT
38	TP53°	<i>na</i>	TP53° + PPP2R1A
39	TP53	WT	<i>na</i>
40	WT	<i>na</i>	<i>na</i>
41	TP53 + HRAS	WT	<i>na</i>
42	TP53	<i>na</i>	CDKN2A
43	CDKN2A + PTEN	<i>na</i>	CDKN2A
44	TP53	<i>na</i>	TP53 + CDKN2A
45	TP53	WT	<i>na</i>
46	WT	WT	<i>na</i>



Table 3 Continued

Patient	primary	lymph node	recurrence
47	TP53 + CDKN2A + HRAS	<i>na</i>	<i>na</i>
48	TP53	WT	<i>na</i>
49	TP53	<i>na</i>	<i>na</i>
50	TP53° + CDKN2A	TP53° + CDKN2A	<i>na</i>
51	HRAS	HRAS	<i>na</i>
52	TP53 + CDKN2A	TP53 + CDKN2A	CDKN2A
53	WT	WT	<i>na</i>
54	TP53	<i>na</i>	WT
55	WT	<i>na</i>	WT
56	WT	<i>na</i>	<i>na</i>
57	TP53°	TP53°	<i>na</i>
58	WT	WT	HRAS
59	WT	<i>na</i>	<i>na</i>
60	WT	WT	<i>na</i>
61	WT	<i>na</i>	WT
62	WT	TP53	WT
63	TP53° + CDKN2A	TP53° + CDKN2A	<i>na</i>
64	WT	WT	<i>na</i>
65	TP53 + CDKN2A	<i>na</i>	<i>na</i>
66	TP53	WT	<i>na</i>

*: part of the assay failed, WT is therefore not 100% sure.

O: a different mutation is detected on the same gene

Germany). Less than 5% of samples were scored differently by the two investigators. These samples were analyzed by a third person working for the software provider company. This way, a consensus mutational typing was reached for all samples.

Sanger sequencing

All solid tumor components were also screened for *TP53* using Sanger sequencing for exon 5-9 as described before (32). The adjacent spindle cell components did not contain enough cells to perform Sanger sequencing, so for these components only MALDI-TOF mass spectrometry was performed.

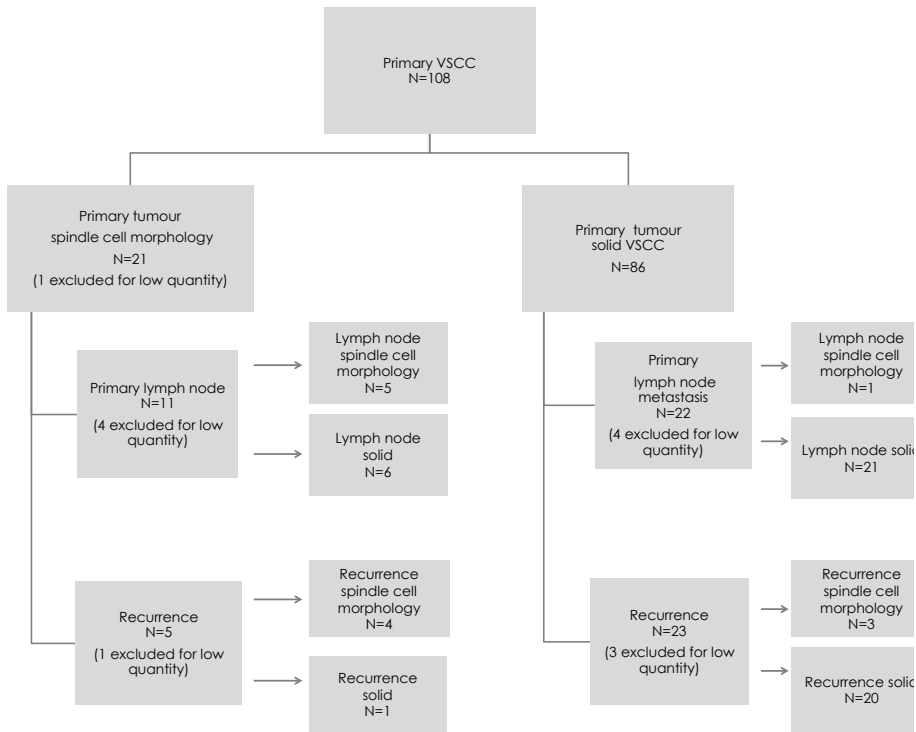


Results

Patients

Of the original cohort of 108 primary VSCCs, 22 were of the VSCC-S subtype of which one was too small for analysis and was excluded. All VSCC-S tumors were HPV negative. Of these primary VSCC-S tumors, 15 (68.2%) patients had lymph

Figure 3 Flowchart on the included primary tumors, lymph node metastases and their adjacent spindle cell components.



Of the original cohort of 108 patients, 22 were of the VSSC-S subtype, of which 1 was excluded for low quantity. Eleven of the VSSC-S and 22 patients of the VSSC subgroup suffered from primary lymph node metastases. 5/11 and 1/22 primary lymph node metastases contained a spindle cell component, respectively.

Five of the VSSC-S and 23 patients of the VSSC subgroup suffered from recurrent disease. 4/5 and 3/20 recurrences contained a spindle cell component, respectively.

node metastasis at time of diagnosis, whereas 26 (30.2%) of the VSCC patients had lymph node metastasis. Thirty-two patients developed recurrent disease (27.3% of VSCC-S vs 30.2% VSCC patients). Eight of the lymph nodes metastases and 4 of the recurrences contained insufficient numbers of tumor cells for our analysis and were excluded from further analysis. Six patients had spindle cell morphology in their lymph node metastasis (5 of which the primary tumor was also of spindle cell morphology), and 8 had a component of spindle cell morphology in their recurrences. In total, 66 patients were included in this study. (Figure 3)

Mutations

TP53 and *CDKN2A* were most frequently mutated in this cohort of primary tumors. The mutations detected in spindle cell morphology components, and in lymph nodes and recurrences are listed in supplemental Table 1. In lymph node metastases and recurrences *TP53* mutations occurred most frequently (10/33 lymph nodes and 8/26 recurrences), followed by *CDKN2A* (5/33 lymph nodes and 7/26 recurrences) and *HRAS* mutations (2/33 lymph nodes and 1/26 recurrences). These mutation frequencies are comparable to those in primary tumors, as described before (32). There was no difference in mutation frequency between VSCCs with and without spindle cell morphology (77 vs 58%, NS).

Recurrences

In two samples of recurrent tumour, the mutation analysis had failed. Thirty-one percent (8/26) of the recurrences showed a similar mutational profile as the primary tumor. (Figure 4 and Table 3) Another 4 (15%) recurrent tumors showed additional mutations compared to the primary tumors, while 10 (38%) recurrent tumors showed to be wild-type for a gene that was found to be mutated in the primary tumor. Four recurrent samples (15%) had simultaneously acquired a new mutation, but at the same time were wild type for a previously mutated gene, when comparing the primary and recurrent tumor.

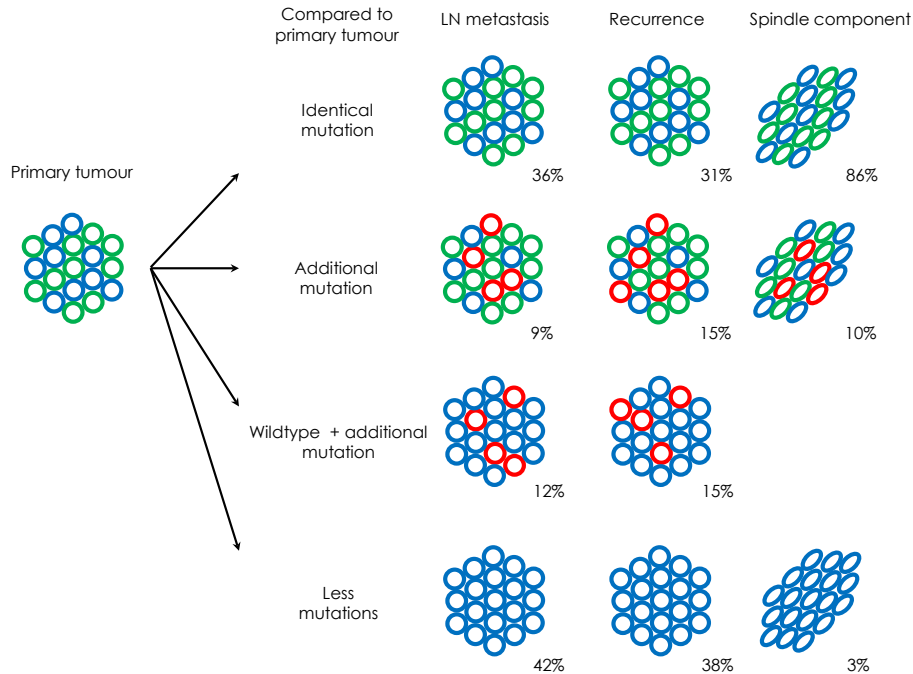
Lymph node metastases

Lymph node metastases more often had the same mutational pattern as the primary tumor, but still 21 out of 33 (64%) of the lymph node metastases had differences in mutations. In fourteen of these (42%) a mutation in the primary tumor was not detected in the lymph node, which most often was *TP53* mutation. Four patients (12%) carried a different *TP53* mutation in their primary tumor than was detected in their lymph node metastases. In lymph nodes metastases from 3 cases (9%) a *TP53* mutation was detected, which was not present in the primary tumor.

Spindle cell components

Sufficient quantities of DNA suitable for somatic mutation analysis could be extracted from 83% (29/35) adjacent spindle cell components and were analyzed for somatic mutations by mass spectrometry. Spindle cell components showed an identical mutational profile as the solid component of the tumor in most cases (86%). In 4 out of 29 cases (14%) the profile differed. In 3 of these, additional mutations were detected in the spindle cell component of the tumor. In one case, the spindle cell component did not show any mutations, whereas the solid component of the tumor did harbor a *TP53* mutation and an *HRAS* mutation. There was no clear correlation between the mutational pattern of the spindle cells and that of the metastases and recurrences.



Figure 4 Schematic representation of comparative mutational profiles

Blue: wildtype, red and green: mutation

Figure 4 shows a schematic illustration of the differences in mutational patterns between primary tumors and spindle cell components, lymph node metastases, and recurrences. Supplemental table 3 shows the full list of detected mutations and supplemental Table 4 shows the DNA content of all FACS-sorted samples.

Discussion

We studied primary, metastatic and recurrent VSCC with spindle variants by targeted sequencing of 14 genes that are most relevant to gynaecological cancers. The results from this study show that VSCC is a disease that can harbour a large variety of mutations, with *TP53*, *CDKN2A* and *HRAS* being most frequently mutated. The spindle cell components appeared to have mutational profiles that are comparable to those of the solid component of primary tumors, so a driver mutation for spindle cell morphology could not be specified. In contrast, lymph node metastases and recurrences showed different mutational profiles compared to their solid primary tumor and spindle cell components. This might reflect the clonal selection

and / or progressive disease that acquires new mutations. Thus, somatic mutation analysis did not identify the spindle cell component as the origin of lymph node metastasis and recurrences. However, the results of this study high light that VSCCs often consist of multiple tumor clones that have different mutational spectra.

A previously published review of the literature on somatic mutations in VSCC has shown that several mutations from different pathways might be affected in VSCC (30). The mutations detected in these cohorts can be attributed to three different pathways: CDKN2A is an upstream regulator in the p53 pathway, PIK3CA, PTEN and PPP2R1A are factors in the PI3K/AKT/mTOR pathway tumor, while HRAS and KRAS are both part of the MAPK/ERK pathway. Each of these pathways is being studied as a possible target for tailored therapy, with differences in success rate (10;19;23-25;29).

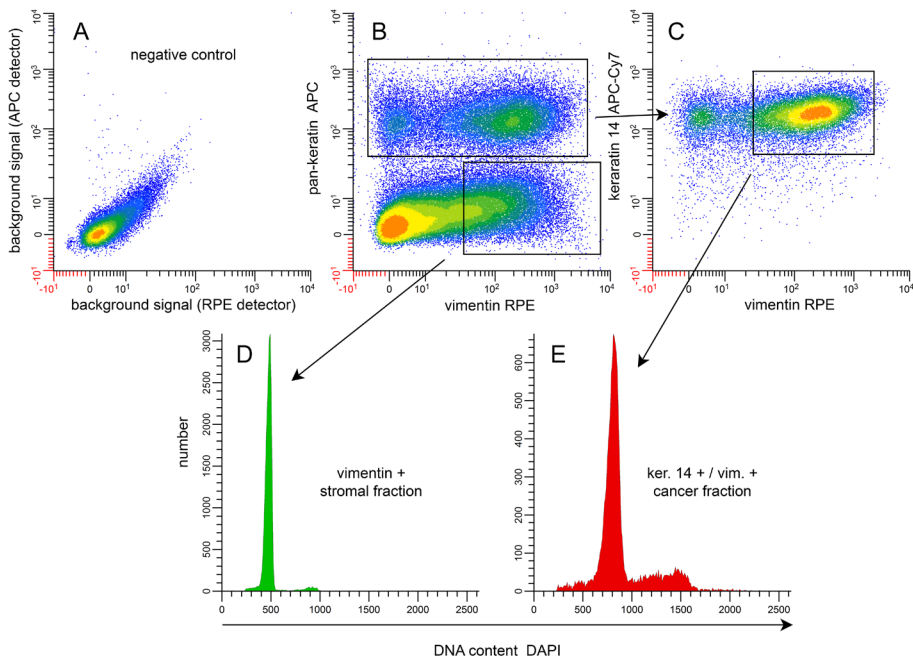
In order to study molecular changes in VSCC-S subpopulations, it was first crucial to discriminate invasive tumor cells from the surrounding stromal tissue. Flow cytometry has proven to be a powerful tool in selecting different subtypes of cells (4), but its application in formalin fixed, paraffin embedded (FFPE) tissue has been limited. In a majority of studies the Hedley method was used which is based on the isolation of single nuclei from FFPE tissue blocks for DNA content analysis. However, in 2005 we published a protocol that enables the simultaneous measurement of keratin-positive carcinoma cells, vimentin-positive stromal cells as well as DNA content (5). Now we extended our protocol with two additional markers allowing a further immunophenotypically dissection of, in this case, FFPE vulvar squamous cell carcinomas into its subpopulations. (Figure 5)

A paradigm in carcinoma metastasis is that epithelial cells undergoing EMT decrease the expression of epithelial proteins such as cadherins, and gain mesenchymal traits such as vimentin expression. Spindle cells have characteristics of EMT, such as loss of cuboid shape and cell-cell junction and frequently express vimentin. Other studies have shown a relationship between upregulated vimentin expression in tumor cells and a worse prognosis (26). In VSCC too, spindle shaped tumor cells are associated with a worse prognosis (31). Here, we have successfully used these phenotypic characteristics to separate spindle cells from the solid tumor component and stromal tissue.

The low cell yield of FACS-sorted spindle cell components impaired the deployment of Sanger sequencing for TP53 analysis on these samples. Thus, TP53 mutation analysis was limited to the solid tumor components only. In this proces of solid tumor Sanger sequencing an estimated 20% of TP53 mutations will be undetected since not all, but only the most frequently mutated exons were sequenced. Another shortcoming of this study might be the fact that targeted sequencing, as we did using mass spectrometry, will always leave *untargeted* genes and mutations undetected. Future developments in mutation analysis techniques will hopefully overcome this problem in investigating low quality and low quantity tumor samples.



Figure 5 Flow cytometry



Flow cytometry of a lymph node metastasis containing spindle cell morphology showing separate cell populations. 4A: negative control. 4B: Cells stained for pancytkeratin and vimentin, with stromal tissue (lower population) negative for keratins and tumor tissue positive for both keratins and vimentin (upper population) 4C: tumor population, with on the right side of the cloud a tumor population expressing vimentin, a marker of epithelial-to-mesenchymal transition. 4D: diploid DNA index from stromal tissue. 4E: aneuploidy DNA index (1.65) from tumor population.



Several studies have shown that primary tumors often consist of multiple clones of tumor cells that, through consecutive alterations in their genome, gain distinctive variations in mutational pattern and metastatic capacity (13;21). Because we collected several tissue biopsies from different locations of the tumors, we have shown that there are many different clones of cancer cells in VSCC. The multiple mutations found in the same tumor do not necessarily reside side-by-side in one cell, but could very well originate from different clones within one tumor. As an example, case nr 53 has both a KRAS and an NRAS mutation that are typically mutually exclusive in tumors. Given the fact that metastases and recurrences often carry less mutations than the primary tumor, these results do imply that recurrences and metastases might arise from a clonal selection from the primary tumor (17). Another hypothesis could be that some of these recurrences are actually new primary tumors. The fact that we have found that nearly 30% of recurrences and nearly 10% of lymph node metas-

tases have acquired additional mutations compared to the primary tumor, might have great implications for the options for targeted therapy. When, in the future, mutations in the primary tumor are targeted by specific therapy, we have to be aware of the risk of selection of tumor cells that represent a different clone with additional, untargeted or yet untargetable mutations. It is therefore crucial to use multimodal anticancer therapies, that block multiple levels of different cancer pathways(35;36).

Although the current adagium in VSCC etiology states that vulvar cancer arises through either an HPV infection or a mutation of the *TP53* gene, our data again show that other mutations such as *CDKN2A* and *HRAS* also play a role in VSCC. The results from the present study show that lymph node metastases and recurrences from VSCC have a broad variety of mutations that are not necessarily of the same profile as the primary VSCC. VSCC-S is not associated with a specific type of mutation or mutated pathway. Also, adjacent spindle cells are likely to have the same mutational pattern as the solid component in the primary tumor. Therefore, somatic mutations are unlikely to be the causing factor for EMT or the origin of VSSC-S. Changes in the TGF-beta pathway through other mechanisms than genetic alterations could be of importance and need to be studied in more detail.

Conclusion

Mutations in *TP53*, *CDKN2A* and *HRAS* were frequently found in primary VSCC, lymph node metastases and recurrences. The results from this study show that VSCCs consist of multiple tumor clones that have different mutational spectra. There is no proof that spindle shaped cells are the origin of lymph node metastasis and recurrences. Future research on targeted therapy is needed, but we should be aware of the risk of clonal selection of cells carrying undetected or untargeted mutations.



Reference List

- (1) Acloque H, Adams MS, Fishwick K, Bronner-Fraser M, and Nieto MA: Epithelial-mesenchymal transitions: the importance of changing cell state in development and disease. *J Clin Invest* 2009, 119:1438-1449
- (2) Ansink A and van der Velde: Surgical interventions for early squamous cell carcinoma of the vulva. *Cochrane Database Syst Rev* 2000,CD002036
- (3) Carless MA and Griffiths LR: Cytogenetics of melanoma and nonmelanoma skin cancer. *Adv Exp Med Biol* 2008, 624:227-240
- (4) Corver WE, ter Haar NT, Dreef EJ, Miranda NF, Prins FA, Jordanova ES, Cornelisse CJ, and Fleuren GJ: High-resolution multi-parameter DNA flow cytometry enables detection of tumor and stromal cell subpopulations in paraffin-embedded tissues. *J Pathol* 2005, 206:233-241
- (5) Corver WE, Ter Haar NT, Dreef EJ, Miranda NF, Prins FA, Jordanova ES, Cornelisse CJ, and Fleuren GJ: High-resolution multi-parameter DNA flow cytometry enables detection of tumor and stromal cell subpopulations in paraffin-embedded tissues. *J Pathol* 2005, 206:233-241
- (6) de Hullu JA and van der Zee AG: Surgery and radiotherapy in vulvar cancer. *Crit Rev Oncol Hematol* 2006, 60:38-58
- (7) de Jong AE, van PM, Hendriks Y, Tops C, Wijnen J, Ausems MG, Meijers-Heijboer H, Wagner A, van Os TA, Brocker-Vriends AH, Vasen HF, and Morreau H: Microsatellite instability, immunohistochemistry, and additional PMS2 staining in suspected hereditary nonpolyposis colorectal cancer. *Clin Cancer Res* 2004, 10:972-980
- (8) Del Pino M, Rodriguez-Carunchio L, and Ordi J: Pathways of vulvar intraepithelial neoplasia and squamous cell carcinoma. *Histopathology* 2013, 62:161-175
- (9) Dittmer C, Fischer D, Diedrich K, and Thill M: Diagnosis and treatment options of vulvar cancer: a review. *Arch Gynecol Obstet* 2012, 285:183-193
- (10) Fouque A, Jean M, Weghe P, and Legembre P: Review of PI3K/mTOR Inhibitors Entering Clinical Trials to Treat Triple Negative Breast Cancers. *Recent Pat Anticancer Drug Discov* 2016, 11:283-296
- (11) Gaarenstroom KN, Kenter GG, Trimbos JB, Agous I, Amant F, Peters AA, and Vergote I: Postoperative complications after vulvectomy and inguinofemoral lymphadenectomy using separate groin incisions. *Int J Gynecol Cancer* 2003, 13:522-527
- (12) Gadducci A, Tana R, Barsotti C, Guerrieri ME, and Genazzani AR: Clinico-pathological and biological prognostic variables in squamous cell carcinoma of the vulva. *Crit Rev Oncol Hematol* 2012, 83:71-83
- (13) Gerlinger M, Rowan AJ, Horswell S, Larkin J, Endesfelder D, Gronroos E, Martinez P, Matthews N, Stewart A, Tarpey P, Varela I, Phillimore B, Begum S, McDonald NQ, Butler A, Jones D, Raine K, Latimer C, Santos CR, Nohadani M, Eklund AC, Spencer-Dene B, Clark G, Pickering L, Stamp G, Gore M, Szallasi Z, Downward J, Futreal PA, and Swanton C: Intratumor heterogeneity and branched evolution revealed by multiregion sequencing. *N Engl J Med* 2012, 366:883-892



- (14) Hennig G, Gehrmann M, Stropp U, Brauch H, Fritz P, Eichelbaum M, Schwab M, and Schroth W: Automated extraction of DNA and RNA from a single formalin-fixed paraffin-embedded tissue section for analysis of both single-nucleotide polymorphisms and mRNA expression. *Clin Chem* 2010, 56:1845-1853
- (15) Judson PL, Habermann EB, Baxter NN, Durham SB, and Virnig BA: Trends in the incidence of invasive and in situ vulvar carcinoma. *Obstet Gynecol* 2006, 107:1018-1022
- (16) Kalluri R and Weinberg RA: The basics of epithelial-mesenchymal transition. *J Clin Invest* 2009, 119:1420-1428
- (17) Klein CA: Selection and adaptation during metastatic cancer progression. *Nature* 2013, 501:365-372
- (18) Kutlubay Z, Engin B, Zara T, and Tuzun Y: Anogenital malignancies and premalignancies: facts and controversies. *Clin Dermatol* 2013, 31:362-373
- (19) Lee JJ, Loh K, and Yap YS: PI3K/Akt/mTOR inhibitors in breast cancer. *Cancer Biol Med* 2015, 12:342-354
- (20) Oonk MH, Hollema H, de Hullu JA, and van der Zee AG: Prediction of lymph node metastases in vulvar cancer: a review. *Int J Gynecol Cancer* 2006, 16:963-971
- (21) Pardoll R, Clarke MF, and Morrison SJ: Applying the principles of stem-cell biology to cancer. *Nat Rev Cancer* 2003, 3:895-902
- (22) Platz CE and Benda JA: Female genital tract cancer. *Cancer* 1995, 75:270-294
- (23) Polager S and Ginsberg D: p53 and E2f: partners in life and death. *Nat Rev Cancer* 2009, 9:738-748
- (24) Porta C and Figlin RA: Phosphatidylinositol-3-kinase/Akt signaling pathway and kidney cancer, and the therapeutic potential of phosphatidylinositol-3-kinase/Akt inhibitors. *J Urol* 2009, 182:2569-2577
- (25) Ripple MO, Kim N, and Springett R: Acute mitochondrial inhibition by mitogen-activated protein kinase/extracellular signal-regulated kinase (MEK) 1/2 inhibitors regulates proliferation. *J Biol Chem* 2013, 288:2933-2940
- (26) Rodrigues IS, Lavorato-Rocha AM, de MM, Stiepcich MM, de Carvalho FM, Baiocchi G, Soares FA, and Rocha RM: Epithelial-mesenchymal transition-like events in vulvar cancer and its relation with HPV. *Br J Cancer* 2013, 109:184-194
- (27) Schrevel M, Gorter A, Kolkman-Uljee SM, Trimbos JB, Fleuren GJ, and Jordanova ES: Molecular mechanisms of epidermal growth factor receptor overexpression in patients with cervical cancer. *Mod Pathol* 2011, 24:720-728
- (28) Spaans VM, Trietsch MD, Crobach S, Stelloo E, Kremer D, Osse EM, Haar NT, van ER, Muller S, van WT, Trimbos JB, Bosse T, Smit VT, and Fleuren GJ: Designing a high-throughput somatic mutation profiling panel specifically for gynaecological cancers. *PLoS One* 2014, 9:e93451
- (29) Tinhofer I, Budach V, Saki M, Kanschak R, Niehr F, Johrens K, Weichert W, Linge A, Lohaus F, Krause M, Neumann K, Endris V, Sak A, Stuschke M, Balermpas P, Rodel C, Avlar M, Grosu AL, Abdollahi A, Debus J, Belka C, Pigorsch S, Combs SE, Monnich D, Zips D, and Baumann M: Targeted next-generation sequencing of locally advanced squamous cell carcinomas of the head and neck reveals druggable targets for improving adjuvant chemoradiation. *Eur J Cancer* 2016, 57:78-86. doi: 10.1016/j.ejca.2016.01.003. Epub: 16 Feb 18.:78-86



- (30) Trietsch MD, Nooij LS, Gaarenstroom KN, and van Poelgeest MI: Genetic and epigenetic changes in vulvar squamous cell carcinoma and its precursor lesions: a review of the current literature. *Gynecol Oncol* 2015, 136:143-157
- (31) Trietsch MD, Peters AA, Gaarenstroom KN, van Koningsbrugge SH, ter Haar NT, Osse EM, Halbesma N, and Fleuren GJ: Spindle cell morphology is related to poor prognosis in vulvar squamous cell carcinoma. *Br J Cancer* 2013, 109:2259-2265
- (32) Trietsch MD, Spaans VM, ter Haar NT, Osse EM, Peters AA, Gaarenstroom KN, and Fleuren GJ: CDKN2A(p16) and HRAS are frequently mutated in vulvar squamous cell carcinoma. *Gynecol Oncol* 2014,10
- (33) van de Nieuwenhof HP, van der Avoort IA, and de Hullu JA: Review of squamous pre-malignant vulvar lesions. *Crit Rev Oncol Hematol* 2008, 68:131-156
- (34) van der Avoort I, Shirango H, Hoevenaars BM, Greffe JM, de Hullu JA, de Wilde PC, Bulten J, Melchers WJ, and Massuger LF: Vulvar squamous cell carcinoma is a multifactorial disease following two separate and independent pathways. *Int J Gynecol Pathol* 2006, 25:22-29
- (35) Xing F, Persaud Y, Pratilas CA, Taylor BS, Janakiraman M, She QB, Gallardo H, Liu C, Merghoub T, Hefter B, Dolgalev I, Viale A, Heguy A, De SE, Cobrinik D, Bollag G, Wolchok J, Houghton A, and Solit DB: Concurrent loss of the PTEN and RB1 tumor suppressors attenuates RAF dependence in melanomas harboring (V600E)BRAF. *Oncogene* 2012, 31:446-457
- (36) Zhou J and Zhang Y: Preclinical development of cancer stem cell drugs. *Expert Opin Drug Discov* 2009, 4:741-752
- (37) zur Hausen H: Papillomaviruses causing cancer: evasion from host-cell control in early events in carcinogenesis. *J Natl Cancer Inst* 2000, 92:690-698



Supplementary tables

Supplemental table 1 *Somatic mutations in spindle cell components*

Patient	primary	spindle primary*	lymph node	spindle lymph node*	recurrence	spindle recurrence*
5	WT	na	na	na	WT	WT
6	WT	WT	WT	na	na	na
8	WT	WT	na	na	na	na
9	WT	na	WT	WT	na	na
13	WT	WT	na	na	na	na
14	WT	na	na	na	WT	CDKN2A + KRAS+ PPP2R1A
17	WT	WT	na	na	WT	WT
24	WT	WT	na	na	na	na
25	WT	WT	WT	na	na	na
26	WT	WT	na	na	na	na
27	CDKN2A	CDKN2A	WT	na	WT	na
36	WT	failed	WT	na	na	na
37	WT	na	na	na	WT	WT
40	WT	failed	na	na	na	na
41	HRAS	WT	WT	WT	na	na
44	WT	WT	na	na	CDKN2A	CDKN2A
47	CDKN2A + HRAS	CDKN2A + HRAS	na	na	na	na
50	CDKN2A	CDKN2A	CDKN2A	na	na	na
51	HRAS	HRAS	HRAS	na	na	na
52	CDKN2A	CDKN2A	CDKN2A	na	CDKN2A	failed
53	WT	CDKN2A + CTNNB1	WT	failed	na	na
56	WT	WT	na	na	na	na
58	WT	na	WT	na	HRAS	failed
62	WT	failed	WT	PTEN	WT	WT
64	WT	na	WT	WT	na	na
65	CDKN2A	CDKN2A	na	na	na	na
66	WT	WT	WT	WT	na	na





Supplemental table 2 Design for GynCarta 2.0 MALDI TOF

GENES (13)	BRAF	CDKN2A	CTNNB1	FBXW7	FGFR2	FGFR3	FOXJ2	HRAS	KRAS	NRAS	PIK3CA	PTEN	PPP2R1A
Mutations	p.V600E	p.R58*	p.D32A	p.R465C	p.S252W	p.R248C	p.C134W	p.G12A	p.G12A	p.G12A	p.R88Q	p.K6fs*4	p.P179L
	p.V600K	p.R58X	p.D32G	p.R465H	p.P253R	p.S249C		p.G12C	p.G12C	p.G12C	p.E542K	p.E7*	p.P179R
	p.V600R	p.R60*	p.D32H	p.R479Q	p.P253L	p.G370C		p.G12D	p.G12D	p.G12D	p.E545A	p.F37S	p.R183G
	p.V600L	p.D108Y	p.D32N	p.R479L	p.Y375C	p.S371C		p.G12R	p.G12F	p.G12R	p.E545G	p.R84G	p.R183W
		p.D108A	p.D32V	p.R505C	p.C382R	p.Y373C		p.G12S	p.G12R	p.G12S	p.E545D	p.R130*	p.R183Q
		p.D108C	p.D32Y		p.N549K	p.A391E		p.G12S	p.G12S	p.G12V	p.E545K	p.R130fs*4	p.S256F
		p.W110*	p.S33A		(T>A)	p.K650E		p.G13C	p.G12V	p.G13A	p.Q546E	p.R130G	p.S256Y
		p.W110X	p.S33C		p.N549K	p.K650Q		p.G13D	p.G13A	p.G13C	p.Q546K	p.R130L	p.W257C
		p.P114L	p.S33F		(T>G)	p.G697C		p.G13R	p.G13C	p.G13D	p.Q546R	p.R130P	p.R258H
		p.P114X	p.S33P		p.K659E			p.G13S	p.G13D	p.G13R	p.Q546P	p.R130Q	
			p.S33Y					p.G13V	p.G13R	p.G13S	p.Q546L	p.R173C	
			p.G34E					p.G13X	p.G13V	p.G13V	p.Y1021C	p.R173H	
			p.G34R					p.Q61H	p.Q61E	p.Q61E	p.T1025A	p.Q214*	
			p.G34V					(C>A)	p.Q61H	p.Q61K	p.T1025X	p.R233*	
			p.S37A					p.Q61H2	(T>A)	p.Q61L	p.M1043I	p.R234W	
			p.S37C					(C>G)	p.Q61H	p.Q61P	(G>A)	p.P248fs*5	
			p.S37F					p.Q61K	(T>G)	p.Q61R	p.M1043I	p.C250fs*2	
			p.S37P					p.Q61L	p.Q61K	p.Q61R	(G>T)	p.K267fs*9	
			p.S37T					p.Q61P	p.Q61L		p.M1043V	p.K267fs*31	
			p.S37Y					p.Q61R	p.Q61P		p.H1047L	p.V290fs*1	
			p.T41A					p.Q61R	p.Q61R		p.H1047R	p.L318fs*2	
			p.T41I								p.H1047Y	p.T321fs*23	
			p.T41N									p.N323fs*2	
			p.T41S									p.N323fs*21	
			p.S45C									p.R335*	
			p.S45F										
			p.S45P										
			p.S45Y										
Total (171)	4	10	28	5	6	9	1	18	19	17	20	25	9
Assays (99)	2	5	12	4	5	8	1	8	7	6	13	22	6

As published in Plos One 2014; Spaans VM, Trietsch MD, Crobach S, Stelloo E, Kremer D, Osse EM, et al. (2014) Designing a High-Throughput Somatic Mutation Profiling Panel Specifically for Gynaecological Cancers. PLOS ONE 9(3): e93451. doi:10.1371/journal.pone.0093451

Supplemental table 3 Full list of information on detected mutations

patient number	primary solid		primary spindle		lymph node solid		lymph node spindle		recurrence solid		recurrence spindle	
	gene	mutation	gene	mutation	gene	mutation	gene	mutation	gene	mutation	gene	mutation
1	CDKN2A		p.R58*		CDKN2A	p.R58*			CDKN2A	p.R58*		
1	PTEN		p.R234W									
1	TP53		p.R273C		TP53	p.R273C			TP53	p.R273C		
2	CDKN2A		p.R80*									
3	KRAS		p.G12V									
3	TP53		p.R248W									
4	TP53		p.T150fs*16		TP53	p.T150fs*16						
5	TP53		p.C135F									
6	TP53		p.C135F									
7	HRAS		p.G12S						CDKN2A	p.R80*		
8	TP53		p.R175H									
9		no mutation detected			TP53	p.Y126fs*10						
10		no mutation detected										
11	HRAS		p.Q61R		HRAS	p.Q61R						
11	PIK3CA		p.E545K									
11	TP53		p.P250L									
12	CDKN2A		p.R80*		CDKN2A	p.R80*						
12	TP53		p.R248W		TP53	p.Y126fs*10						
13	TP53		p.G245S									
14		no mutation detected							TP53	p.R175H	CDKN2A	p.R58X
14											KRAS	p.G12S
14											PPP2R1A	p.S256Y
15		no mutation detected										
16		no mutation detected										
17	TP53		p.R175H									





Supplemental table 3 Continued

patient number	primary solid	primary spindle	lymph node solid		lymph node spindle		recurrence solid		recurrence spindle	
18	HRAS	p.G13D								
19	no mutation detected						CDKN2A	p.R80*		
19							TP53	p.R248Q		
20	no mutation detected		TP53	p.G279E						
21	CDKN2A	p.R80*								
21	HRAS	p.G13R								
21	TP53	p.P151S								
22	TP53	p.R248Q								
23	CDKN2A	p.R80*								
23	TP53	p.R273C								
24	TP53	p.R175H								
25	TP53	p.R273C	TP53	p.R273C						
25			HRAS	p.G13R						
26	TP53	p.E287D								
26	TP53	p.E294X								
27	CDKN2A	p.R80*								
28	PPP2R1A	p.R258H						CDKN2A	p.R80*	
28	TP53	p.P152L								
28	TP53	p.R248Q								
29	no mutation detected									
30	HRAS	p.G12S								
30	PIK3CA	p.E545K								
30	TP53	p.R273C								
31	TP53	p.R249S								
32	TP53	p.R273C								

Supplemental table 3 Continued

patient number	primary solid	primary spindle	lymph node solid	lymph node spindle	recurrence solid	recurrence spindle
33	PIK3CA p.H1047Y				PIK3CA p.H1047R	
33	PPP2R1A p.R258H					
34	HRAS p.G13S					
34	TP53 p.R273H				TP53 p.R248W	
35	TP53 p.D259H					
36	no mutation detected					
37	TP53 p.G245S					
37	TP53 p.V216M				TP53 p.R213Q	
38	TP53 p.C176X				PPP2R1A p.R183Q	
38	TP53 p.G266E					
39	no mutation detected	KRAS p.G13S				
40	HRAS p.G12S					
41	TP53 p.G245S					
41	TP53 p.V173G					
42	TP53 p.D186fs ins TAGC				CDKN2A p.R80*	
43	failed for all assays					
44	TP53 p.V157F	PTEN p.R173H			TP53 p.V157F CDKN2A p.R58*	
44	TP53 p.P190L				CDKN2A p.R58*	
45	TP53 no mutation detected		PIK3CA p.E542K			
46	CDKN2A p.W110*	CDKN2A p.W110*				
47	HRAS p.G12S	HRAS p.G12S				
47	TP53 p.V203L					
48	TP53 p.V173L					





Supplemental table 3 Continued

patient number	primary solid		primary spindle		lymph node solid		lymph node spindle		recurrence solid		recurrence spindle	
49	TP53	p.R248W	CDKN2A	p.R58*	CDKN2A	p.R58*	CDKN2A	p.R58*				
50	CDKN2A	p.R58*			TP53	p.R181C						
50	TP53	p.N267fs*3	HRAS	p.G12D	HRAS	p.G12D						
51	HRAS	p.G12D			CDKN2A	p.R80*	CDKN2A	p.R80*	CDKN2A	p.R80*	KRAS	p.G13S
52	CDKN2A	p.R80*	CDKN2A	p.R80*	TP53	p.R273C			PPP2R1A	p.R258H		
52	TP53	p.R273C			CDKN2A	p.R58*		KRAS				
53	no mutation detected		CTNNB1	p.S37Y				NRAS				
53	TP53	p.S241Y										
54	TP53	p.S241Y										
55	no mutation detected											
56	no mutation detected											
57	TP53	p.D148N			TP35	p.P142S						
57	TP53	p.R282W			TP53	p.R248Q						
58	no mutation detected											
59	no mutation detected											
60	no mutation detected											
61	no mutation detected											
62	TP53	p.R248Q			TP53	p.R248Q		PTEN		p.R130fs*4		
62	TP53	p.V172I			TP53	p.P142S						
63	CDKN2A	p.R58*			CDKN2A	p.R58*						
63	TP53	p.E294X			TP53	p.E294X						
64	no mutation detected											
65	CDKN2A	p.R80*	CDKN2A	p.R80*								
65	TP53	p.R273H										
66	TP53	p.C135X										

Supplemental table 4 *Copy number alterations*

Patient	primary	spindle primary	lymph node	spindle lymph node	recurrence	spindle recurrence
5					aneuploid	aneuploid
6	aneuploid	aneuploid				
8	aneuploid	aneuploid				
9			aneuploid	aneuploid		
13	aneuploid	diploid + aneuploid				
14					aneuploid	diploid
17	failed	aneuploid			aneuploid	aneuploid
24	diploid	diploid				
25	diploid + aneuploid	diploid				
26	diploid	diploid				
27	diploid	diploid				
36	diploid + aneuploid	aneuploid				
37					diploid + aneuploid	diploid + aneuploid
40	aneuploid	diploid				
41	failed	aneuploid	diploid + aneuploid	failed		
44	aneuploid	aneuploid			aneuploid	diploid + aneuploid
47	diploid + aneuploid	aneuploid				
50	aneuploid	aneuploid				
51	aneuploid	diploid				
52	aneuploid	aneuploid			diploid + aneuploid	aneuploid
53	aneuploid	aneuploid	aneuploid	aneuploid		
56	diploid + aneuploid	aneuploid				
58					aneuploid	aneuploid
62	aneuploid	diploid + aneuploid	aneuploid	diploid + aneuploid	diploid	aneuploid
64			aneuploid	aneuploid		
65	aneuploid	diploid				
66	aneuploid	aneuploid	diploid + aneuploid	aneuploid		

